Skeletal Radiol (1995) 24:7–12

Skeletal Radiology

Pigmented villonodular synovitis: MRI characteristics

T.H. Hughes, F.R.C.R.[1], D.J. Sartoris, M.D.[1], M.E. Schweitzer, M.D.[2], D.L. Resnick, M.D.[1]

[1] Department of Radiology, University of California, San Diego and Veterans Administration Medical Center, San Diego, California, USA
[2] Department of Radiology, Thomas Jefferson University Hospital, Philadelphia, Pennsylvania, USA

Abstract. The magnetic resonance imaging (MRI) scans of 26 patients with histopathologically proven pigmented villonodular synovitis (PVNS), involving joints but excluding tendon sheaths, were reviewed retrospectively. The purpose of this study is to define the spectrum and frequency of MRI characteristics for PVNS using conventional spin echo (in two cases before and after intravenous administration of gadopentate dimeglumine) and also gradient echo techniques. A cystic variety is presented, the MRI appearances of which have not been found in a review of the literature.

Key words: Pigmented villonodular synovitis – Magnetic resonance – Cystic arthropathy

"Pigmented villonodular synovitis" (PVNS), "bursitis," and "tenosynovitis" are designations coined by Jaffe et al. [1] in 1941 to encompass a host of descriptive terms ("xanthoma," "giant cell tumor," "xanthogranuloma") previously used to describe an uncommon synovial proliferative lesion which may affect tendon sheaths, less commonly joints, and rarely bursae. As the name implies, the proliferation may be either villous or nodular or a combination of the two. The most frequent presentation is a nodular variety commonly seen in the tendon sheaths, principally on the volar aspect of the phalanges, which almost universally is well circumscribed, affecting only a small area of the synovium. This variety is also referred to as "giant cell tumor of tendon sheath" (GCT), due to the presence of numerous multinucleated giant cells, or as "localized nodular tenosynovitis." The present article concentrates on the less common arthropathy, which usually affects the knee, hip, ankle, glenohumeral, and elbow joints, in descending order of frequency [2].

Correspondence to: David J. Sartoris, M.D., Department of Radiology –114, Veterans Administration Medical Center, 3350 La Jolla Village Drive, San Diego, CA 92161-9114, USA

There are several well-recognized characteristics of PVNS as seen on magnetic resonance imaging (MRI), including: low signal on both T1- and T2-weighted images due to hemosiderin deposition and thick fibrous tissue, presence of "fat" signal within the mass due to clumps of lipid laden macrophages, hyperplastic synovium, bone erosions in those joints with insufficient intra-articular space for outward proliferation of the synovium (particularly the hip), and preservation of bone density as well as joint space [3–9]. We evaluated 26 patients with PVNS arthropathy to determine the frequency of these characteristics, identify cystic change within the proliferative mass, and observe signal characteristics with various spin and gradient echo sequences using differing main field strengths as well as intravenous gadolinium enhancement, the use of which is mentioned in only one previous report [10].

Materials and methods

We reviewed the MRI scans and other imaging studies that were available for 26 patients (13 men, 13 women; age range 13–68 years; average age 39 years), all with histopathologically proven PVNS, from the teaching museum at the Veterans Hospital in San Diego. The joints involved were 20 knees, 2 hips, 1 talonavicular joint, 1 proximal tibiofibular joint, 1 lumbar facet joint, and 1 trapeziometacarpal joint. A total of 111 MRI sequences were reviewed – 31 T1-weighted (TR/TE: 1000-499/80-50), 29 proton-density-weighted (TR/TE: 3100-1200/40-15), 33 T2-weighted (TR/TE. 3100-1200/120-60), 3 T1-weighted following intravenous administration of gadopentate dimeglumine (Gd-DTPA), (TR/TE: 886-18/15-4.6), and 15 with various gradient echo sequences (TR 1000-75, TE 25-10, flip angle 5°–180°) – with reference to:

1. Presence of bony erosions.
2. Localized or diffuse nature of the mass.
3. Overall signal intensity of the synovial mass with respect to muscle. Presence of a synovial mass "capsule," septations, and clumps of tissue within the mass and their relative signal intensity.
4. Degree of heterogeneity of the synovial mass.
5. Presence of edema, either in the bones or the surrounding soft tissues.
6. Continuity of the adjacent joint cartilage.

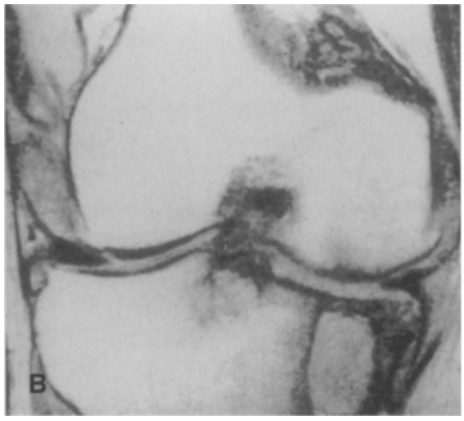

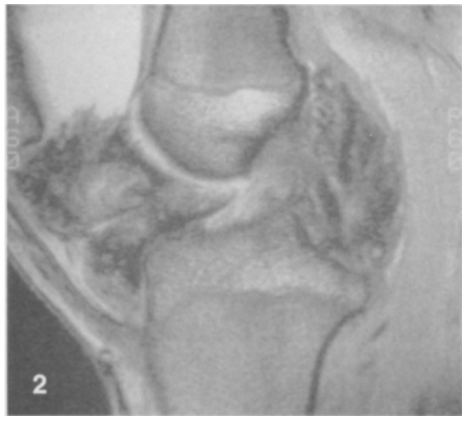

Fig. 1. A Frontal plain roentgenogram of the knee to demonstrate erosions. **B** Corresponding coronal T1-weighted (TR 1000, TE 40) magnetic resonance (MR) image demonstrating the bone erosions. (Courtesy of T. Cope, M.D., San Diego, California, USA)

Fig. 2. Sagittal gradient echo image (TR 1000, TE 15, flip angle 90°, MPGR acquisition) of the knee showing the low signal seen due to the paramagnetic effect of hemosiderin. (Courtesy of M. Schweitzer, M.D., Philadelphia, Pennsylvania, USA)

7. Presence of focal fluid collections (cysts) within the synovial mass.
8. Clarity of the margins of the synovial mass.
9. Presence of a joint effusion.

Scans were obtained at the following field strengths (tesla): 0.3, 0.35, 0.5, 1.0, 1.5. Comparison was made between the different field strengths to assess the effect this would have on image contrast, in particular with reference to magnetic susceptibility of hemosiderin. Scans were reviewed in an unblinded fashion. One of the 26 patients has previously been presented in the literature in a case report [11].

Results

The results of the investigation were as follows:

Bone erosions/subchondral synovial tissue or cysts: These were detected in 12 of the 20 knees (Fig. 1), both hips, the lumbar facet joint, and the proximal tibiofibular joint, but not in the ankle or trapeziometacarpal joint. In all patients, the main determining factor for ease of erosion visibility was the scan plane rather than the sequence used.

Localized or diffuse nature of the mass: Of the 20 knees, 14 had diffuse synovial proliferation, 4 localized, and in 2 the image was equivocal. In the other joints, it was not possible to ascertain by which of the two mechanisms the proliferation started, because the joint was full of "tumor" due to the restricted space within the joint.

Overall signal intensity of the synovial mass with respect to muscle. Presence of a synovial mass "capsule", septations, and clumps of tissue within the mass and their relative signal intensity: The overall signal intensity of the synovial mass was decreased with gradient echo sequences (Fig. 2), in comparison with the other sequences in which generally the mass showed either decreased or the same signal as that of muscle and only occasionally exhibited increased intensity.

On approximately half of the 111 sequences, the process demonstrated a capsule around some of its borders that was of decreased signal intensity compared to muscle (Fig. 3). Only 2 showed increased signal intensity, and in approximately half, a capsule was not visible or was of the same signal as muscle. There were no great differences among the sequences with respect to these findings. Approximately two-thirds of the sequences showed septa of decreased signal (Fig. 4) and in one-third septa were not visible. A few sequences demonstrated septa of increased signal intensity or a mixture of increased and decreased intensity. The gradient echo sequences showed more septa of decreased intensity. The synovial mass contained many focal clumps of tissue of differing signal intensities; generally these were of decreased signal intensity (Fig. 5), or a mixture of increased and decreased intensity (Fig. 6). The gradient echo images had proportionally more low signal in the clumps. With regard to individual patients, a capsule, septa, or clumps were visible on some sequences and not others, and showed variability in signal intensity between sequences.

Heterogeneity of the mass: Using a scale of 0 (homogeneous) to 3 (very heterogeneous), the overall signal from the synovial mass was assessed. The enhanced T1-weighted images produced the greatest overall tissue heterogeneity, followed by, in decreasing order, the gradient echo, T2, proton density and T1 images. The expected increase in heterogeneity of the synovial mass with increasing field strength was not observed; indeed, comparing the two large groups, the mean of the 0.5-tesla group was 1.7 and that of the 1.5-tesla group 1.5.

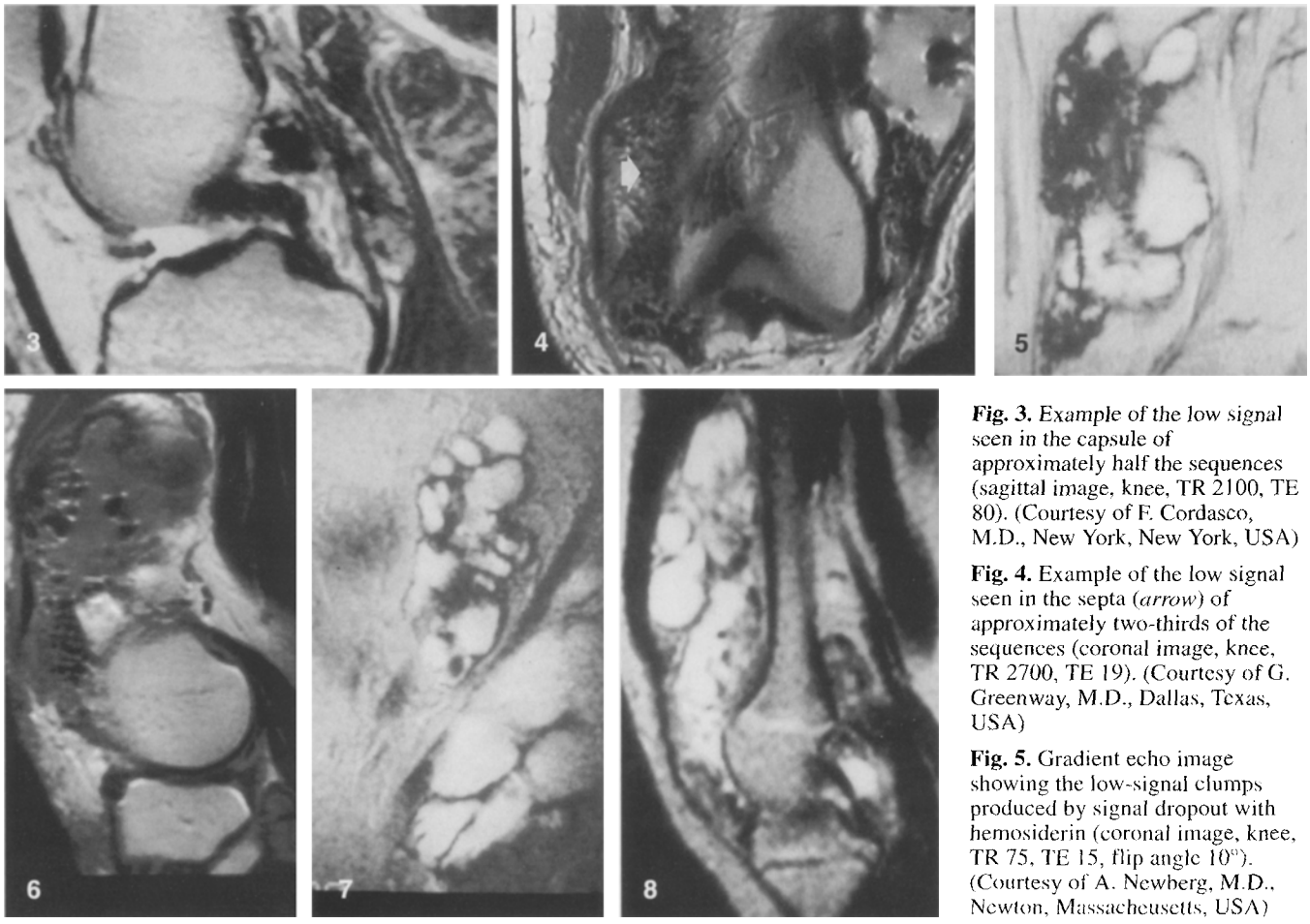

Fig. 3. Example of the low signal seen in the capsule of approximately half the sequences (sagittal image, knee, TR 2100, TE 80). (Courtesy of F. Cordasco, M.D., New York, New York, USA)

Fig. 4. Example of the low signal seen in the septa (*arrow*) of approximately two-thirds of the sequences (coronal image, knee, TR 2700, TE 19). (Courtesy of G. Greenway, M.D., Dallas, Texas, USA)

Fig. 5. Gradient echo image showing the low-signal clumps produced by signal dropout with hemosiderin (coronal image, knee, TR 75, TE 15, flip angle 10°). (Courtesy of A. Newberg, M.D., Newton, Massacheusetts, USA)

Edema: Edema was seen in six patients, either in the bone adjacent to an erosion or in the nearby soft tissues (T1-weighted, five sequences; T2-weighted, three sequences). All patients with detectable edema had prominent erosions, subchondral synovial tissue, or cysts.

Cartilaginous defects: Although specific cartilage sequences were not used, 53 sequences showed no cartilage defects and in 16 the cartilage was not fully visualized. Twenty-nine sequences (8 patients) showed focal defects. In any particular patient, if a focal cartilage defect was present, it was visible on nearly all sequences. All of these patients had erosions. Thirteen sequences demonstrated generalized cartilage thinning, but the average patient age in this subset was 57 years.

Presence of focal fluid collections (cysts): Eleven patients had cysts within the synovial proliferation, and seven of these also had effusions. Although such cysts could represent joint fluid that has become encysted, two masses appeared distinctly cystic (Figs. 7, 8).

Clarity of margins: Eighty-one sequences showed clear margins and the rest were obscure. There was no observable difference among the various sequences.

Effusion: Fluid was detectable in 19 of the 20 knees and the ankle but not in any of the other joints.

Fig. 6. Mixed clumps of high and low signal due to lipid and hemosiderin respectively (sagittal image, knee, TR 417, TE 11). (Courtesy of G. Greenway, M.D., Dallas, Texas, USA)

Fig. 7. Example of a principally cystic mass (sagittal image, knee, TR 2000, TE 100). (Courtesy of R. Stiles, M.D., Atlanta, Georgia, USA)

Fig. 8. Example of a principally cystic mass (sagittal image, knee, TR 3100, TE 80). (Courtesy of A. Newberg, M.D., Newton, Massacheusetts, USA)

Findings following Gd-DTPA administration: Although Gd-DTPA was employed in only two cases (three sequences), in these cases a notable increase in overall heterogeneity was observed and a trend towards an increase in overall, capsule, and septae signal intensity was seen.

Discussion

Due to the nature of the film museum, which represents many cases from outside hospitals, several of the sequences were not complete but tended to represent the films of interest, thus introducing potential sample bias (49 complete, 62 incomplete). In addition, a wide variety of pulse sequences was reviewed, hence statistical analysis was not performed. With its high resolution and excellent soft tissue contrast, MRI has become the imaging

method of choice for the diagnosis of soft tissue tumors and synovial masses. Initial hopes that MRI would allow specific diagnoses preoperatively have not been fulfilled, except in regard to occasional lesions such as PVNS [12–14], considered difficult to diagnose by computed tomography (CT) [15], although some reports indicate no clear advantage of MRI over CT in defining synovial lesions [16].

A review of the literature shows that the synovial mass of PVNS is usually grape-like [16] and heterogeneous [3, 11, 17], with an overall signal intensity that is either isointense or decreased compared to that of muscle [3, 12], or, occasionally, increased on T2-weighted images due to edema [5, 14, 18]. However, we found that the appearance varies widely, depending on the relative proportions of lipid, hemosiderin, fibrous stroma, septation, pannus formation, fluid, cyst formation, and cellular elements.

Usually dispersed within the proliferative mass are clumps of hemosiderin, which has a paramagnetic (ferromagnetic [19]) effect, causing signal dropout. This phenomenon is enhanced by high field strength [5, 19] and T2* relaxation seen when gradient refocusing is used (Figs. 2, 6), especially on heavily T2*-weighted images. The reason for this was initially explained by Gomori et al. [20] in an MR-study of developing brain hematomas. These investigators found a ring of low signal intensity around the edge of the hematoma, corresponding to hemosiderin deposition in macrophages. This is caused by preferential T2 proton relaxation enhancement by the heterogeneity in the local magnetic susceptibility, produced by the hemosiderin that was in the ferric (Fe^{3+}) state, and hence decreased T2 relaxation in nearby water molecules, causing diminished signal. The effect is proportional to the square of the magnetic field and as such should be more pronounced at high field strengths. However, signal dropout and hence overall heterogeneity did not increase with increasing field strengths in our series, possibly reflecting decreased T1 tissue contrast at high field strength counteracting the signal dropout due to the paramagnetic effect. Hypointensity may also be seen on T1-weighted images due to this phenomenon if the T2 is shortened to a value lower than the acquisition TE of the T1-weighted images, producing a T2 effect on T1-weighted images. However, sometimes no signal dropout is observed on any sequence [18].

Collections of lipid-laden macrophages (foam cells) appear as focal areas of high signal with T1 weighting and intermediate signal with T2 weighting, and these collections occasionally may be dominant with regard to signal intensity in the MR images.

Subdividing the lesion are septa, which probably represent the edges of individual nodules pushed together and buried within the mass. These usually are of low signal intensity and may show signal dropout at high field strength or on gradient echo images, due to a combination of both fibrosis and hemosiderin. The edge of the lesion usually is well demarcated by a low signal intensity capsule [5, 11, 17], again due to either fibrosis [5] or hemosiderin [6].

The previously reported incidences of bone erosions about the knee in PVNS detectable by routine radiography range from 26% [2] to 32% [21]. Our series showed a 60% incidence of detectable erosions by MRI, which may reflect increased sensitivity of this method. As in previous series [8], the erosions contained a mixture of low and high signal intensity tissue on both T1- and T2-weighted images, indicating not only fluid but other elements of synovial proliferation.

MRI findings in localized and diffuse PVNS may be similar in many respects, reflecting the marked histologic overlap between the two varieties of lesion [10]. Although the clarity of the margins with T2 imaging previously was thought to allow classification as localized or diffuse [6], in two of our cases at the knee and all those in other joints the images were equivocal on this point, reflecting the fact that in tight joints, once the process has reached a certain size its origins can no longer be ascertained, and that within the knee a large lesion has the same effect. The presence of an effusion aids in the differentiation.

As in previous reports [8], most (19/20) of our patients with lesions in the knee had a joint effusion. Fluid was not seen in tighter joints, probably reflecting elevated intra-articular pressure. The two patients who showed a predominance of focal fluid collections within the proliferative mass both had joint effusions. This finding therefore may represent fluid that had become encysted, as the mass grew in a fronded manner. Unlike other patients, who had the occasional cyst within the synovial proliferation, the masses in these two were distinctly cystic.

Prior to injection of Gd-DTPA intravenously, both joint effusion and inflamed synovium show the same signal intensity on both T1- (low) and T2- (high) weighted images [22]. However, in a T1-weighted image obtained immediately after the intravenous injection of Gd-DTPA, the synovium enhances, thus allowing its differentiation from fluid. In one case report [10], Gd-DTPA was thought to aid in the identification of PVNS nodules and thus help in delineating the mass. In our series, the enhanced T1-weighted images had the greatest signal heterogeneity, thus helping to define the lesions.

Apart from diagnosis, MRI also is useful in defining the extent of disease [23], because the ligaments, tendons, menisci, and cartilage are visualized in addition to the lesion. A detailed map of the disease within the joint is thus constructed [8]. Steinbach et al. [8] have illustrated the regular finding of involvement posterior to the cruciate ligaments and in synovial cysts within the popliteal fossa in cases of PVNS. Hence treatment can be both planned [6, 8, 17, 24] and monitored [6, 8, 25]. Earlier diagnosis [6] may allow the choice of a less extensive procedure [26]. The use of Gd-DTPA is thought to be valuable in assessing surgical planning, by more fully defining the lesion [10]. MRI can on occasions depict PVNS which cannot be directly visualized at arthroscopy [23], and as such should always be used when there is a clinical suspicion of PVNS or a patient presents with symptoms and signs of the condition.

MRI has proven useful in defining the extent of recurrent disease following surgery [27] and in monitoring regression with yttrium-90 silicate [28] therapy. As biopsy in cases of PVNS may provide tissue containing young stromal cells, suggesting the presence of a malignant neoplasm (e.g., synovial sarcoma) [29], MRI prior to definitive surgery is advisable.

Within the differential diagnosis for PVNS when imaged with MRI are several conditions. Synovial osteochondromatosis has a multiple target appearance with low-signal-intensity peripheral rims and isointense or signal-reflecting fat in the center. Rheumatoid arthritis tends to show thinner synovial proliferation of more even thickness, although it may occasionally be fronded and contains less hemosiderin. Synovial sarcoma tends to have a shorter T1 and longer T2 in comparison, and signal dropout due to calcification may be observed. In hemophilia there is an absence of fatty components due to an absence of foam cells. Lipoma arborescens, on the other hand, is markedly fatty and fronded and of more intermediate signal, and may fill and expand the joint to a greater degree.

Conclusions

The appearance of PVNS on MRI is not pathognomonic but is strongly suggestive of the diagnosis if the typical features are present. MRI may aid routine radiology in the diagnosis of PVNS. Whatever the method of treatment, MRI is useful in preoperative planning and postoperative monitoring for recurrence. Awareness of the variable MRI appearances of this condition may assist in distinguishing it from other causes of monoarticular arthritis, such as idiopathic synovial osteochondromatosis, intracapsular osteoid osteoma, and septic arthritis.

A typical case of PVNS imaged with MRI is likely to show: – Erosions, no matter which joint – A diffuse mass in a loose joint capsule such as the knee – A heterogeneous mass, possibly with a low-signal-intensity capsule and probably low-signal-intensity septae and small clumps of tissue with variable signal intensity

Occasionally bone marrow edema and focal cartilage defects may be seen, but only when erosions are present. The mass occasionally has a predominantly cystic appearance. An effusion is a regular finding.

Acknowledgments. We would like to thank the following for the kind donation of their films to the musculoskeletal teaching museum at the Veterans Administration Hospital in San Diego: J. Brown, M.D., St. Louis, Missouri, USA. T. Cope, M.D., San Diego, California, USA. T. Burkhard, M.D., San Diego, California, USA. V. Chandrani, M.D., Honolulu, Hawaii, USA. M. Reicher, R. Christiansin, M.D., San Diego, California, USA. F. Cordasco, M.D., New York, New York, USA. S. Fernandez, M.D., Frontera, Mexico. G. Greenway, M.D., Dallas, Texas, USA. R. Kerr, M.D., Los Angeles, California, USA. J. Krammer, M.D., Vienna, Austria. A. Newberg, M.D., Newton, Massacheusetts, USA. M. Pathria, M.D., San Diego, California, USA. R. Stiles, M.D., Atlanta, Georgia, USA.

References

1. Jaffe HL, Lichtenstein L, Sutro CJ. Pigmented villonodular synovitis, bursitis and tenosynovitis. Arch Pathol Lab Med 1941; 31: 731–765.
2. Dorwant RH, Genant HK, Johnston WH, Morris JM. Pigmented villonodular synovitis of synovial joints: clinical, pathologic and radiologic features. AJR 1984; 143: 877–885.
3. Jelinek JS, Kransdorf MJ, Utz JA, Hudson-Berry, B Jr, Thompson JD, Heekin RD, Radowich MS. Imaging of pigmented villonodular synovitis with emphasis on MR imaging. AJR 1989; 152: 337–342.
4. Khoury GM, Shimkin PM, Kleinman GM, Mastroianni P, Nijensohn DE. Computed tomography and magnetic resonance imaging findings of pigmented villonodular synovitis of the spine. Spine 1991; 16: 1236–1237.
5. Kottal RA, Vogler JB, Matamoros A, Alexander AH, Cookson JL. Pigmented villonodular synovitis: a report of imaging in two cases. Radiology 1987; 163: 551–553.
6. Poletti SC, Gates III HS, Martinez SM, Richardson WJ. The use of magnetic resonance imaging in the diagnosis of pigmented villonodular synovitis. Orthopedics 1990; 13: 185–190.
7. Spritzer CE, Dalinka MK, Kressel HY. Magnetic resonance imaging of pigmented villonodular synovitis: a report of two cases. Skeletal Radiol 1987; 16: 316–319.
8. Steinbach LS, Neumann CH, Stoller DW, Mills CM, Crues Jr III, Lipman JK, Helms CA, Genant HK. MRI of the knee in diffuse pigmented villonodular synovitis. Clin Imaging 1989; 13: 305–316.
9. Wetzel LH, Levine E. Soft tissue tumors of the foot: value of MR imaging for specific diagnosis. AJR 1990; 155: 1025–1030.
10. Besette PR, Cooley PA, Johnson RP, Czarnecki DJ. Gadolinium-enhanced MRI of pigmented villonodular synovitis of the knee. J Comput Assist Tomogr 1992; 16: 992–994.
11. Kerr R. Diffuse pigmented villonodular synovitis. Orthopedics 1989; 12: 1008–1012.
12. Kransdorf MJ, Jelinek JS, Moser, Jr RP, Utz JA, Brower AC, Hudson TM, Berrey BH. Soft tissue masses: diagnosis using MR imaging. AJR 1989; 153: 541–547.
13. Suh J, Griffiths HJ, Galloway HR, Everson LI. MRI in the diagnosis of synovial disease. Orthopedics 1992; 15: 778–781.
14. Sundaram M, McGuire MH, Fletcher J, Wolverson MK, Heiberg E, Shields JB. Magnetic resonance imaging of lesions of synovial origin. Skeletal Radiol 1986; 15: 110–116.
15. Sundaram M, Chalk D, Merenda J, Verde JN, Salinas-Madrigal L. Case report 563. Skeletal Radiol 1989; 18: 433–435.
16. Boyd AD Jr, Sledge CB. Evaluation of the hip with pigmented villonodular synovitis. A case report. Clin Orthop 1992; 275: 180–186.
17. Sartoris DJ, Mink JH, Kerr R. The foot and ankle. In: Mink JH, Deutsch AL, eds. MRI of the musculoskeletal system: a teaching file. New York: Raven Press, 1990: 424–427.
18. Sher M, Lorigan JG, Ayala AG, Libshitz HI. Case report 578. Skeletal Radiol 1990; 19: 131–133.
19. Weissman BN, Hussain S. Magnetic resonance imaging of the knee. Rheum Dis Clin North Am 1991; 17: 637–68.
20. Gomori JM, Grossman RI, Goldberg HI, Zimmerman RA, Bilaniuk LT. Intracranial hematomas: imaging by high-field MR. Radiology 1985; 157: 87–93.
21. Smith JH, Pugh DG. Roentgenographic aspects of articular pigmented villonodular synovitis. AJR 1962; 87: 1146–1156.
22. Kursunoglu-Brahme S, Riccio T, Weisman MH, Resnick D, Zvaifler N, Sanders ME, Fix C. Rheumatoid knee: role of gadopentetate-enhanced MR imaging. Radiology 1990; 176: 831–835.
23. Mandelbaum BR, Grant TT, Hartzman S, Reicher MA, Flannigan B, Bassett LW, Mirra J, Finerman AM. The use of

MRI to assist in the diagnosis of pigmented villonodular synovitis of the knee. Clin Orthop 1988; 231: 135–139.
24. Stiehl JB, Hackbath DA. Recurrent pigmented villonodular synovitis of the hip joint, case report and review of the literature. J Arthroplasty 1991; 6: S85–S90.
25. Gumpal JM, Shawe DJ. Diffuse pigmented villonodular synovitis: non-surgical management. Ann Rheum Dis 1991; 531–533.
26. Johansson JE, Ajjoub S, Coughlin LP, Wener JA, Cruess RL. Pigmented villonodular synovitis of joints. Clin Orthop 1982; 163: 159–166.
27. Weisz GM, Gal A, Kitchener PN. Magnetic resonance imaging in the diagnosis of aggressive villonodular synovitis. Clin Orthop 1988; 236: 303–306.
28. Chen DY, Lan JL, Chou SJ. Treatment of pigmented villonodular synovitis with yttrium-90: changes in immunologic features, Tc-99 uptake measurements, and MR imaging of one case. Clin Rheumatol 1992; 11: 280–285.
29. Klompmaker J, Veth RPH, Robinson PH, Molenaar WM, Nielsen HKL. Pigmented villonodular synovitis. Arch Orthop Trauma Surg 1990; 109: 205–210.